

# High-quality ZnO films grown by atmospheric pressure metal–organic chemical vapor deposition

Li Wang, Yong Pu, Wenqing Fang, Jiangnan Dai, Yufeng Chen, Chunlan Mo, Fengyi Jiang\*

*Education Ministry Engineering Research Center for Luminescent Materials and Devices, Nanchang University, 330047, P.R. China*

Received 7 November 2004; received in revised form 22 April 2005; accepted 14 May 2005

Available online 29 June 2005

Communicated by R. James

## Abstract

High-quality ZnO films grown by atmospheric pressure metal–organic chemical vapor deposition (AP-MOCVD) are demonstrated in this paper. Surface morphology, structural quality and optical properties of the as-grown films were investigated by AFM, double-crystal XRD and photoluminescence (PL) measurements. The effect of buffer layers grown at different temperature on the film quality was studied. It was found that the low-temperature buffer layer was effective to improve the surface morphology, but was not effective to improve the structural quality. On the other hand, the high-temperature buffer layer can greatly improve the structural quality, but yields a relatively rougher surface. Both the samples deposited using either a low-temperature or high-temperature buffer layer showed strong UV luminescence at room-temperature. A fine structure of free excitons was observed at 11 K in the sample with a high-temperature buffer layer.

© 2005 Elsevier B.V. All rights reserved.

PACS: 81.15. Gh; 78.55 –m; 68. 55 –a

Keywords: A1. Dislocation density; A1. Exciton; A3. MOCVD; B1. ZnO

## 1. Introduction

For a long time, ZnO was well-known as a phosphorescent powder and polycrystalline varistor material. Since the discovery of room-

temperature ultraviolet lasing from nanostructured ZnO thin films [1], ZnO has also been recognized as a promising ultraviolet laser material. Its large exciton binding energy (59 meV) [2] in principle favors efficient room-temperature excitonic emission. In addition, the band-gap energy of ZnO can be extended to 4 eV by adding Mg or Mn and narrowed to 2.8 eV by alloying

\*Corresponding author.

E-mail address: [jiangfy@vip.163.com](mailto:jiangfy@vip.163.com) (F.Y. Jiang).

with CdO [3], indicating its high potential for use in many applications, especially for light-emitting devices.

For ZnO film growth, numerous deposition techniques including molecular beam epitaxy (MBE) [1,4], sputtering [5], pulse-laser deposition (PLD) [6] and MOCVD [7,8] have been employed. Among these techniques, MOCVD has many advantages for volume production, and it has proved to be an excellent growth technique for III–Vs, especially for the nitrides. In addition, investigations have revealed that atmospheric pressure growth of GaN films usually yields larger grain size and higher mobility than low-pressure growth [9–11]. So, AP-MOCVD is a promising way to grow high-quality ZnO films. However, there have been only a few investigations of AP-MOCVD growth of ZnO films reported in the literature [12–15]. The problem for MOCVD growth of ZnO is that Zn precursors are highly reactive with O precursors (usually oxygen or water), so that pre-reaction in the gas phase occurs easily and usually produces white powder on the substrate. The problem will be more serious for atmospheric pressure growth. However, we found this problem can be solved through optimizing the reactor structure and growth conditions. In this paper, growth of high-quality ZnO films by AP-MOCVD is demonstrated.

## 2. Experimental details

ZnO films were grown by a homemade vertical AP-MOCVD system. Fig. 1 shows a schematic

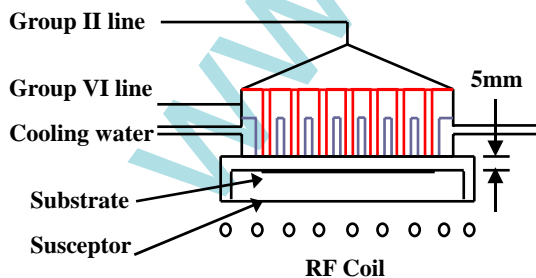


Fig. 1. Schematic diagram of the reactor for the AP-MOCVD system.

diagram of the reactor. To reduce the pre-reaction, the reactor was designed so that the group II and VI reactant gases were delivered separately and mixed at only 5 mm above the substrate surface, as shown in the diagram. Meanwhile, a large flow rate carrier gas (15 L/min) was used to obtain a high gas velocity. The susceptor was rotating during the growth to get a good uniformity of the films. Two inch *c*-plane sapphire was used as the substrate. DEZn and H<sub>2</sub>O were used as the Zn and O precursors, respectively. Three samples were grown in this study. Sample A was grown with no buffer layer, while samples B and C were grown with a low-temperature (LT) and a high-temperature (HT) buffer layer, respectively. The LT buffer layer was grown at 160 °C and the HT buffer layer at 680 °C. The buffer layers were annealed at 850 °C for 6 min before growing the epi-layers. The epi-layers of all the three samples were grown at 680 °C. The growth time was 1 h, and the films thickness was 3 μm.

The contact-mode AFM (Benvuan Nano Instrument, China) measurements were performed under ambient conditions. XRD rocking curves of the films were measured using a double-crystal X-ray diffractometer (QC200, BEDE Instruments, UK). Cu K $\alpha$  line was used as the source and Ge (004) was used as the monochromator. Photoluminescence spectra of the films were measured at room temperature and 11 K, using the 325 nm line of a He–Cd laser as the excitation source.

## 3. Results and discussion

Fig. 2 shows AFM images of the three samples. In Fig. 2(a), a very rough surface of sample A can be seen. It is clearly shown that the film was formed by stacking of many large grains, and several holes can be seen between the grain boundaries. The scan area for Fig. 2(a) is 10 μm × 10 μm, and the RMS roughness is 96 nm. For sample B, which was grown using a LT buffer layer, a very smooth surface can be seen (see Fig. 2b). The RMS roughness is 2.5 nm across an area of 30 μm × 30 μm. As has been elucidated in GaN research, during the LT buffer layer growth a high density of nuclei will form on the substrate

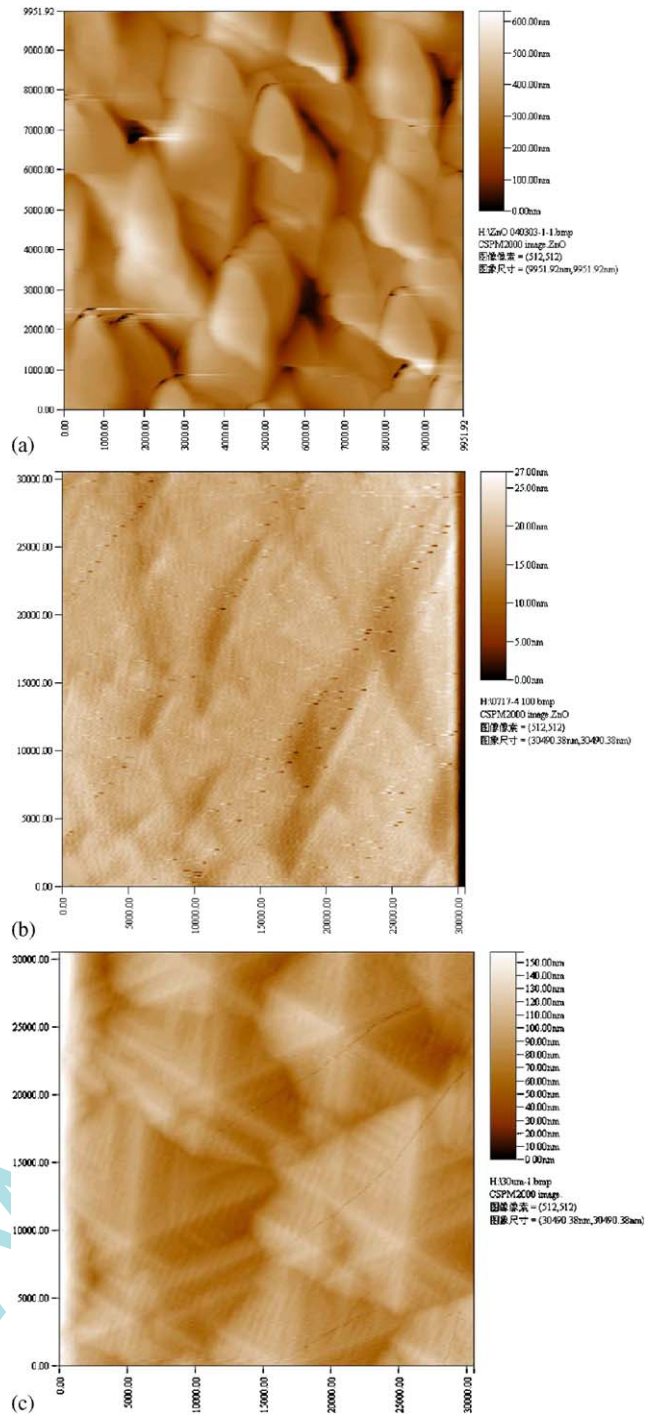


Fig. 2. AFM images of the three samples. (a) Sample A, 10  $\mu\text{m} \times 10 \mu\text{m}$ . (b) Sample B, 30  $\mu\text{m} \times 30 \mu\text{m}$ . (c) Sample C, 30  $\mu\text{m} \times 30 \mu\text{m}$ .

and a quasi-two-dimensional (2D) growth can be obtained after the coalescence of the nuclei, which result in the smooth surface [16]. However, many etch pits can be seen on the surface in the AFM image of sample B, suggesting a high dislocation density in the film. To obtain larger grain size and lower dislocation density, it is necessary to decrease the nucleation density [17]. One simple way to do that is by increasing the nucleating temperature. But as has been shown in sample A, directly nucleating at 680 °C will lead to 3D growth and result in discrete grains. To obtain a smooth surface, an annealing step was introduced in the growth procedure of sample C. After depositing the nucleation layer at 680 °C, we annealed it at 850 °C for 6 min. Fig. 2(c) shows the AFM image of sample C for a scan area of 30  $\mu\text{m} \times 30 \mu\text{m}$ . Very large hexagonal grains with uniform orientation can be seen in the image. The mean diameter of the grains is larger than 10  $\mu\text{m}$ . The RMS roughness across this area is 17 nm, which is larger than sample B but much smaller than sample A. The improvement of the surface morphology can be explained by the migration of the surface atoms and the release of stress during the annealing.

It is well-known that heteroepitaxial layers grown on largely lattice-mismatched substrates usually exhibit a high density of dislocations, which is the major cause of the broadening of XRD rocking curves [18]. For wurtzite crystals such as ZnO and GaN, the screw dislocation has a Burgers vector  $b = [001]$ , and the edge dislocation has a Burgers vector  $b = 1/3[110]$ . Their densities can be deduced from the FWHM of a symmetric and an asymmetric XRD scan. So the FWHM of (002) and (102)  $\omega$ -rocking curves can be used as the indicators of screw and edge dislocations [19]. Fig. 3 shows the rocking curves of the three samples. In Fig. 3(a), both (002) and (102) reflections of sample A show broad line widths, suggesting both a high screw dislocation density and a high edge dislocation density. With an LT buffer layer, sample B showed a significantly narrowed (002) line width in Fig. 3(b), but its (102) rocking curve was broadened. As pointed out in the above discussion, a high density of nuclei will form on the substrate when an LT

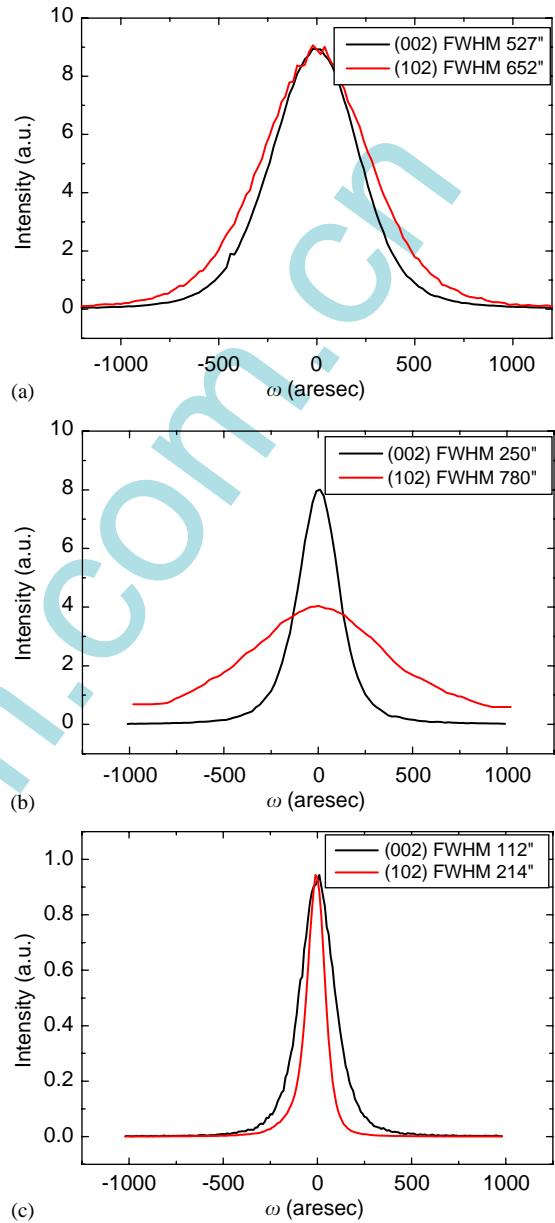


Fig. 3. Rocking curves of the samples for both (002) and (102)  $\omega$ -scan. (a) Sample A (b) sample B (c) sample C

buffer layer is used and a quasi-2D growth can be achieved. The quasi-2D growth leads to improvement of the out-of-plane orientation, i.e., narrowed (002) line width. But the high density of nuclei will result in small grain sizes, which cause a

high density of edge dislocations, because the edge dislocations usually formed at the grain boundaries. That is the possible reason for broadening of the (102) rocking curve of sample B. Sample C, which was grown using an HT buffer layer, and shows very large grain sizes in the AFM image. In agreement with the AFM result, the rocking curves shown in Fig. 3(c) also have very small line width. The FWHM of the (002) and (102) rocking curves are 112 and 214 arcsec, respectively. These are the smallest values so far obtained for ZnO films directly grown on sapphire by MOCVD, to the best of our knowledge. This result suggests that the HT buffer layer is very effective to improve the structural quality of ZnO films.

To compare the optical properties of the films grown using LT and HT buffer layers, PL spectra of samples B and C were measured at both room temperature and low temperature. Fig. 4(a) shows a room-temperature PL spectrum. It can be seen that both the samples have a strong UV emission at 3.28 eV. This peak is the transition of free excitons with LO phonon replicas, which has been confirmed by the temperature-dependent PL measurements [20]. A very weak “green peak” can be seen in the spectrum of sample B. The origin of this peak is still in dispute, but it was usually attributed to the emission related to native point defects such O vacancy and  $O_{Zn}$  [21]. For sample C, the green peak was absolutely absent, suggesting that the HT buffer can effectively suppress the formation of native point defects in ZnO films. Fig. 4(b) shows the 11 K PL of the two samples. A peak at 3.365 eV dominates both the spectra of samples B and C. This is the emission of an exciton bound to a neutral donor [20]. At the higher energy side, three peaks are shown clearly at 3.375, 3.385 and 3.419 eV, respectively. The peak at about 3.385 eV shows only a shoulder, so the position is a roughly estimated one. The energy positions of these three peaks are very close to the A, B and C free excitons observed in optical reflectance spectra of bulk ZnO crystal [2]. So they are tentatively attributed to the free A, B and C excitons. The slight red shift of these peaks compared to bulk ZnO can be explained by a tensile strain in the films. It should be noticed that

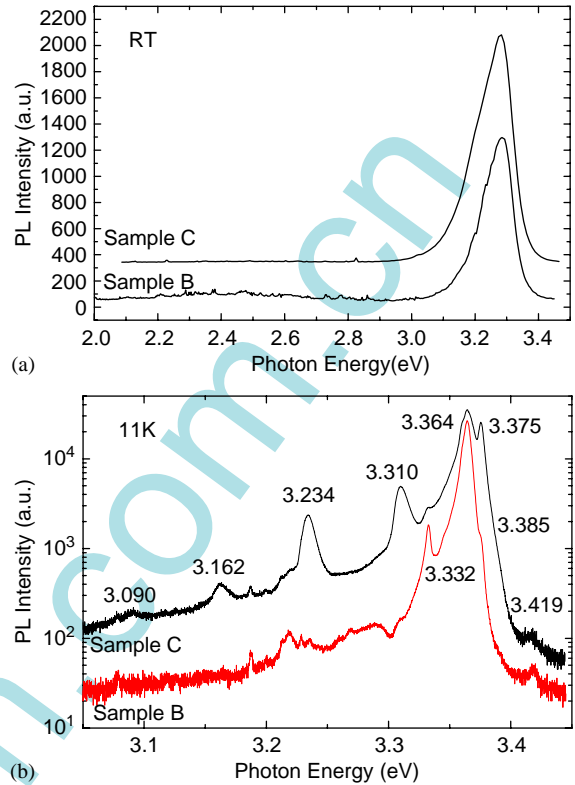


Fig. 4. PL spectra of samples B and C measured at (a) room temperature and (b) 11 K.

the peak at 3.419 eV could also be attributed to the first excited state of the A exciton. So a more detailed analysis is needed to clarify the origin of this peak. But it is indisputable that the appearance of either the C exciton or the excited A exciton strongly suggest the high quality of the films, because only the A and B excitons have been observed in previously reported PL spectra for ZnO films heteroepitaxially grown on sapphire. At the lower energy side, sample B shows three peaks. The peak at 3.332 eV has been attributed to a two-electron transition in the literature [22]. The two weak peaks at 3.291 and 3.219 eV are attributed to the 1LO and 2LO phonon replicas of the bound exciton, because they have an energy difference multiple of the LO phonon for ZnO (72 meV) [23]. For sample C, the two-electron transition line was greatly decreased together with the bound exciton line, while a clear structure of the free exciton's LO

phonon replicas appears. The intensity ratio of exciton A to the bound exciton of sample B and sample C are 0.07 and 0.72, respectively. The stronger free exciton emission in sample C further proves the effectiveness of the HT buffer layer to suppress the formation of native defects in the ZnO films.

In summary, high-quality ZnO films have been successfully grown by AP-MOCVD with a novel reactor. The effect of buffer layers on the film properties has been studied. The results show that: (1) LT buffer layer is very effective to improve the surface morphology, but it is not effective to improve the structural quality; (2) Using a HT buffer layer, the structural quality can be greatly improved, but the surface of the film will be relatively rougher; (3) The film grown using an HT buffer layer shows stronger free exciton emission than that grown with an LT buffer layer, and a fine structure of free excitons was observed in the sample grown using an HT buffer layer.

### Acknowledgements

This work was supported by 863 project (Grant no. 2003AA302160) and the Electronic information technology development fund.

### Reference

- [1] Z.K. Tang, G.K.L. Wong, P. Yu, *Appl. Phys. Lett.* 72 (1998) 3270.
- [2] D.G. Thomas, *J. Phys. Chem. Solids* 15 (1960) 86.
- [3] T. Fukumura, Z. Jin, A. Ohtomo, H. Koinuma, M. Kawasaki, *Appl. Phys. Lett.* 75 (1999) 3366.
- [4] D.M. Bagnall, Y.F. Chen, Z.Q. Zhu, T. Yao, S. Koyama, M.Y. Shen, T. Goto, *Appl. Phys. Lett.* 70 (1997) 2230.
- [5] K.H. Bang, D.K. Hwang, J.M. Myoung, *Appl. Surf. Sci.* 207 (2003) 359.
- [6] A. Ohtomo, K. Tamura, K. Saikusa, K. Takahashi, T. Makino, Y. Segawa, H. Koinuma, M. Kawasaki, *Appl. Phys. Lett.* 75 (1999) 2635.
- [7] W.I. Park, S.J. An, G.C. Yi, H.M. Jiang, *J. Mater. Res.* 16 (2001) 1358.
- [8] N. Oleynik, A. Dadgar, J. Christen, J. Blasing, M. Adam, *Phys. Stat. Sol. (A)* 192 (2002) 189.
- [9] D.D. Koleske, A.E. Wickenden, R.L. Henry, M.E. Twigg, J.C. Culbertson, *Appl. Phys. Lett.* 73 (1998) 2019.
- [10] F.A. Ponce, *MRS Bull.* 22 (1997) 51.
- [11] S. Einfeldt, T. Bottcher, S. Figge, D. Hommel, *J. Crystal Growth* 230 (2001) 357.
- [12] Y. Kashiwaba, F. Katahira, K. Haga, T. Sekiguchi, H. Watanabe, *J. Crystal Growth* 221 (2000) 431.
- [13] S. Bethke, H. Pan, B.W. Wessels, *Appl. Phys. Lett.* 52 (1988) 138.
- [14] B.P. Zhang, Y. Segawa, K. Wakatsuki, Y. Kashiwaba, *Appl. Phys. Lett.* 79 (2001) 3953.
- [15] C.R. Gorla, N.W. Emanetoglu, S. Liang, W.E. Mayo, Y. lu, *J. Appl. Phys.* 85 (1999) 2595.
- [16] H. Amano, I. Akasaki, K. Hiramatsu, N. Koide, N. Sawaki, *Thin Solid Films* 163 (1988) 415.
- [17] J. Han, T.B. Ng, R.M. Biefeld, M.H. Crawford, D.M. Follstaedt, *Appl. Phys. Lett.* 71 (1997) 3114.
- [18] Y.J. Sun, O. Brandt, T.Y.L.A. Trampert, K.H. Ploog, *Appl. Phys. Lett.* 81 (2002) 4928.
- [19] B. Heying, X.H. We, S. Keller etc, *Appl. Phys. Lett.* 68 (1996) 643.
- [20] S.W. Jung, W.I. Park, H.D. Cheong, G.C. Yi, H.M. Jang, *Appl. Phys. Lett.* 80 (2002) 1924.
- [21] Bixia Lin, Zhuxi Fu, Yunbo Jia, *Appl. Phys. Lett.* 79 (2001) 943.
- [22] D.C. Look, C. Coskun, B. Clafin, G.C. Farlow, *Physica B* 340-342 (2003) 32.
- [23] C. Klingshirm, *Phys. Stat. Sol. (B)* 71 (1975) 547.